

Biomimetic Transmembrane Nanopores Using DNA Nanotechnology

Ezry Santiago-McRae

March 8, 2022

Contents

1 Overview and Objectives	3
2 Background	4
2.1 General Background	4
2.2 Anchoring DNA Nanostructures to Synthetic Membranes	4
2.3 Inclusion Morphology	5
2.4 Nanopores - Transport and Gating	5
3 Significance	6
4 Preliminary Work	7
4.1 DNA Nanostructures	7
4.2 Synthetic Vesicles	7
4.3 Modeling and Simulation	8
5 Aim 1: Anchoring	9
5.1 Introduction and Summary	9
5.2 Research Design	10
5.3 Outline of Steps	12
5.3.1 Aim 1.1: Select and Parameterize	12
5.3.2 Aim 1.2: Use FEP	12
5.4 Expected Outcomes	13
5.5 Potential Problems and Alternative Approaches	13
6 Aim 2: Morphology	14
6.1 Introduction and Summary	14
6.2 Research Design	14
6.3 Outline of Steps	15
6.3.1 Aim 2.1: Design the Inclusions with DNA	15
6.3.2 Aim 2.2: Compare morphology stability and permeability	15
6.3.3 Aim 2.3: Estimate free energies of insertion using FEP	15
6.4 Expected Outcomes	16
6.5 Potential Problems and Alternative Approaches	16
7 General Computational Methods	16
7.1 Molecular Dynamics	16
7.1.1 General Description	16
7.1.2 Specifics	16
7.2 Free Energy Perturbations	17
7.2.1 General Description	17

7.2.2	Specifics	17
7.3	Metadynamics	18
7.3.1	General Description	18
7.3.2	Specifics	19
8	Timeline	19

1 Overview and Objectives

The goal of the proposed research is to predict the stability of DNA-nanostructures inserted in synthetic membranes. This will be a function of prosthetic group identity and number, nanostructure geometry, and membrane composition.

Biomedical nanotechnologies apply a wide range of nanomaterials, each with unique strengths and weaknesses. This project will focus on the interface of two nanotechnologies: nucleic acids, which are highly addressable with well-defined intermolecular interactions; and lipid (and lipid-like) vesicles, which are inexpensive, robust, and can transport a large payload. Though powerful and useful independently, combining these unique features into a single platform would open new avenues of research into therapeutics which would be highly specific, potent, and robust such as the delivery of anti-cancer drugs such that side-effects are minimized. Additionally, by leveraging the self-assembly of lipid bilayers and DNA nanotechnology, these therapeutics may be produced at relatively low cost and in greater volumes when compared to other nanotechnologies.

Unfortunately, DNA-membrane hybrid structures are fundamentally unstable due to the free energy costs of forming and maintaining close interactions between DNA (a polyanion) and an amphipathic bilayer (even with positively charged head groups). This challenge is usually addressed by covalently attaching hydrophobic prosthetic groups to the DNA. While this approach has found some success, experimental optimization remains expensive and time-consuming. Therefore, the proposed research will focus on computational methods for comparing prosthetic groups allowing us greater control, higher-throughput, and higher resolution than a purely experimental approach. Both quantitative and qualitative comparisons will be made.

Aim 1: Identify optimal prosthetic groups to anchor DNA origami structures in synthetic membranes

The free energy of insertion is a quantitative measure of a nanostructure's stability in the inserted versus free state. This is, in turn, related to the probability of insertion by the Boltzmann distribution. Alchemical free-energy perturbation methods will be used to calculate the relative free energy of insertion of DNA nanostructures with different prosthetic groups.

Specific Sub-Aims:

- 1.1 Select and parameterize candidate prosthetic groups using CGenFF and manual analogy
- 1.2 Use FEP methods to calculate relative free energies of insertion into at least three model membranes (POPC, POPC:DOPC:Chol, PBD-b-PEG) for each prosthetic group

Aim 2: DNA Nanostructure Design

The geometry of the inclusion and the arrangement of the prosthetic groups will also influence the efficiency of insertion and the stability (free energy) of the final system. Both free energy perturbations and enhanced sampling techniques will be adapted to these computations. Using the results from aim 2, DNA origami structures will be designed and both coarse-grained and all-atom simulations will be carried out to compare geometry stability and examine the effects on the membranes. Prosthetic group identity, number, and location will also be compared.

Specific Sub-Aims:

- 2.1 Design several membrane inclusions using a combination of DNA origami and prosthetic groups based on natural membrane inclusions.
- 2.2 Simulate these geometries using both coarse-grained and all-atom models to assess basic stability and permeability of the inclusion-membrane systems
- 2.3 Compare the relative free energies of insertion of each inclusion nanostructure, varying the number and positions of prosthetic groups.

2 Background

2.1 General Background

DNA nanotechnology is the interdisciplinary application of nanoengineering principles to DNA-based structures and machines. DNA, well-known as the carrier of genetic information, has many appealing features for nanoengineering including biocompatibility, well-defined self-assembly mechanisms, both rigid and flexible motifs, inexpensive synthesis, good stability, and straight-forward conjugation chemistry [16]. Several design paradigms are employed in the field - origami, which use a plasmid as a scaffold folded by shorter staple strands; bricks, which are made of several short strands which then assemble into larger structures (DNA 'LEGO'); and single stranded structures dominated by sequence effects (e.g. strand displacement circuits, aptamers, DNAzymes, etc.) [14, 41]. Because of these features, nucleic acid nanotechnology (including RNA, DNA, and nucleic acid analogues) has immense potential in biomedical applications as diagnostic tools[41], drug delivery systems [8] and even as novel therapeutics [40].

Just as DNA nanotechnology is the repurposing of DNA, **synthetic vesicles** are made of engineered plasma membranes. These vesicles are frequently used experimentally as model membranes but also have potential as drug delivery systems in their own right [26, 11]. Their main strengths are their low cost, good biocompatibility, and ability to transport relatively large volumes of small molecules either in their lumen or in the hydrophobic core of the bilayer itself [26, 11]. These features are distinct from other delivery systems which have prohibitively low cargo volumes (DNA origami) or questionable biocompatibility [43]. Unlike DNA nanotechnology, however, synthetic vesicles are paradigmatically less diverse, consisting primarily of amphipathic molecules in a liquid bilayer with limited intrinsic functionalization; they are usually functionalized with biogenous membrane proteins or nanoparticles.

Hybrid nanotechnology is any nanotechnology which combines two or more nanomaterial classes or design paradigms. Combining synthetic vesicles with DNA nanotechnology, as in our case, is a rapidly growing field of research due to the potential for novel therapeutics and eventual applications in synthetic biology [8, 7, 4, 26, 12, 11]. However, DNA, a hydrophilic polyanion, is poorly suited to being in direct contact with the lipophilic center of a lipid bilayer [10].

2.2 Anchoring DNA Nanostructures to Synthetic Membranes

To address the **problem of combining hydrophilic DNA with amphipathic bilayers** - especially the hydrophobic core - researchers have attempted a wide range of heteromolecular "prosthetic groups" which introduce lipophilic side chains to the otherwise lipophobic DNA [12]. These prosthetic groups can, in theory, be any sufficiently lipophilic small molecule, but only a subset of all possible prosthetic groups have been tested [12, 19]. These experiments, though essential, are held back by the challenge and expense of synthesizing the novel chimeric molecules [19]. Even when DNA-prosthesis chimeras can be synthesized problems persist: transmembrane DNA structures tend to induce poration of the membrane permitting small molecules to cross and lipids to flip-flop, amphipathic DNA nanostructures can aggregate in solution [7, 31, 38].

An **ideal prosthetic group**, then, would avoid membrane disruptions, have manageable levels of aggregation in aqueous solution, and require less than 10 such modifications (due to the cost of production). That said, several metrics are currently in use to assess the value of a particular prosthetic group including membrane permeability of the ligated DNA, attachment rates, leakage rates of vesicle contents, cytotoxicity, DNA assembly yields, and amphipathic DNA aggregation [38, 10, 4]. Trends are difficult to discern because most comparisons between prosthetic groups are confined to one or a few classes of molecules (e.g. lipids [15, 47], porphyrins [2, 42]). As a result, broad trends are difficult to discern [20].

Fortunately, humans are not the first to consider using biopolymers to functionalize lipid bilayers - the diversity of **natural transmembrane proteins** is an invaluable library of stable, functional nanostructures which interface stably and compatibly with the cell membrane. Functionally, these membrane proteins act as interfaces between the cell's internal and external environments; transporting nutrients, ions, and other small molecules into and out of the cell [30]. Mechanistically, insertion of transmembrane proteins can be achieved either at the time of synthesis or post-synthesis [32, Chapter 20]. Structurally, their amino acid sequences and folding patterns create a belt or domain of hydrophobic residues which stabilize the protein in the interior of the membrane while hydrophilic residues face the cytosol or aqueous environment [32,

Chapter 20]. This simplistic description belies the nuanced roles played by individual amino acids in the stability of transmembrane polypeptides and proteins [13].

Unlike the engineering problem of DNA-functionalized synthetic vesicles, biological transmembrane structures have evolved under particular **selective pressures** - having energetic, chemical, spatial, and temporal constraints; a living thing is limited in its resources and must allocate them carefully [32]. In contrast, our energetic and temporal constraints are negligible and our spatial and chemical constraints are very different. Spatially, living things are capable of placing hydrophobic residues as frequently as required [30] whereas each prosthetic group incurs an additional cost for us. Chemically, living things are restricted to the handful of naturally occurring hydrophobic amino acids whereas we may consider the vast universe of organic compounds[19].

Nevertheless, the **principles gleaned from biological systems** may yet be of use; the WALP and KALP synthetic model peptides, for example, are based on the observation that aromatic residues reside preferentially at the hydrophobic-hydrophilic interface while small, flexible hydrophobic residues are most often observed within the hydrophobic domain [23]. In this vein, Burns, Stulz, and Howorka have implemented ethyl-phosphorothioate modified DNA nanostructures in which the anionic oxygen of the phosphate-sugar backbone with an acyl chain connected by a sulfur atom [9]. They were able to insert the DNA barrels using alternating voltage, but high voltages either damaged or ejected the nanostructures [9]. They and others had similar findings using just two to six porphyrin anchors [6]. These experiments have suggested the utility of a biomimetic approach, but necessarily deviate in their use of single prosthetic group identities and limited modification numbers.

2.3 Inclusion Morphology

By **inclusion or nanostructure morphology** we mean both the surface shape and distribution of physical-chemical parameters (e.g. charge, polarizability, hydrophobicity, etc.). In the context of transmembrane DNA nanotechnology, topologies are frequently rectilinear (rectangular or hexagonal prisms [14], tee-shaped [25], or stepped [12]) while parameter distributions are dominated by the negatively charged backbone punctuated by two or more prosthetic groups [12, 8]. Quantitative comparisons tend to treat morphologies as categorical variables rather than continuous ones [6]. While larger hydrophobic domains show improved stability in the membrane, the non-specific "leakiness" of the pores remains an issue [12]

Biological membrane inclusions (e.g. transmembrane proteins) do indeed exhibit important morphological traits: 1) as noted, they universally possess hydrophobic belts which stabilize them in the hydrophobic core of the membrane, but vary in the content, thickness, and topology of that belt; 2) their extra- and intracellular domains may be functionalized to interact with other nanostructures, the membrane, molecules in solution, or other parts of the same nanostructure; and 3) the overall topologies are highly variable but are specific to the nanostructure's membrane environment and function including curvature (matching or inducing), thickness, and electrostatics [32, 30]. While porins and channels tend to possess roughly cylindrical or conical morphologies, signalling, anti-toxin, motility, and membrane-fusion/fission proteins are much more structurally diverse, including long appendages, catalytic centers, multiple conformations, and signal-transduction mechanisms [32]. Classification of naturally occurring transmembrane proteins relies primarily on sequence-function and phylogenetic considerations [36, 17]. Less common are classification schemes which include surface features explicitly [21] which is of central importance in the proposed work.

Biological systems, though understandable as modular compositions, are not intrinsically separable; that is, any modularity is applied by researchers in an effort to better understand the whole. In contrast, nanotechnological systems are modular *by design* making it possible to treat topology and surface features independently - which is not possible for biological evolution. Nevertheless, our control of DNA nanostructures is not infinitely fine being constrained to a very small set of primary and secondary structures [16]. As a consequence, our ability to mimic biological transmembrane morphologies is, at least superficially, limited - requiring novel approaches to design and optimization.

2.4 Nanopores - Transport and Gating

In the broadest sense, a **nanopore** is a physical opening from one to several nanometers across. These are fundamental in both biological and industrial systems for sorting, purifying, sensing, and transporting

molecules. Though conceptually simple, nanopores (both natural and artificial) display remarkable diversity in size, shape, and mechanical and chemical properties [18]. Nanopores may be classified by material, substrate, or application [18, 39, 34]. DNA nanopores are frequently designed using DNA origami but can also be as simple as a six-helix bundle [7, 4]. They are sometimes further functionalized with prosthetic polypeptides [7].

The **basic qualities of any nanopore** include the rate at which it transports its substrate and the specificity with which it does so. In biological and biomimetic systems, pore size tends to be less than a few nanometers with overall nanostructures ranging from several nanometers to tens of nanometers across [18].

There are several classes of biological transmembrane transporters, organized based on their substrate, gating, and mode of action [32, 35]. By substrate, transporters are broadly classed as anion, cation, small molecule, water, or general transporters. By gating, transporters can be controlled by ligand, pH, voltage, cofactor, or chemical gradient [32]. Finally, by mode of action, transporters can be passive or active; uniport, symport, or antiport; and, if active, powered by chemical gradients or ATPase activity [32]. Although active transport has, so far, eluded DNA nanotechnologists, there have been considerable efforts toward gated DNA nanopores including voltage, pH, and ligand/cofactor gating [11, 18]. Leakiness and poor specificity are persistent problems in these systems [18, 5].

Ion channels are an attractive target for DNA nanotechnologists due to the natural selectivity of the polyanionic backbone for cationic substrates [1]. Ion channels differ from other transporters in several ways that make them useful models; 1) their selection mechanisms are relatively well understood [30], 2) as passive transporters, their mode of action is simple [30], and 3) over 1,500 structures have been curated in the Transporter Classification Database [35], often with ligands bound providing insight into mechanisms and modes of action. Considerable progress has been made in recent years toward selective, efficient DNA-based ion channels [44, 37, 24].

Several mechanisms exist by which ion channels and nanopores more generally can be gated including conformational changes [27], blocking structures (e.g. [29], Figure 1), and quaternary structural changes (e.g. [22]). Signal transduction is either by discrete shifts from closed to open [30] or by higher-level stabilization of the open or closed state (ELIC)[45]. Reproduction of these mechanisms in DNA nanotechnology frequently focus on strand displacement and aptamer-based mechanisms which remove some blocking strand(s) [28].

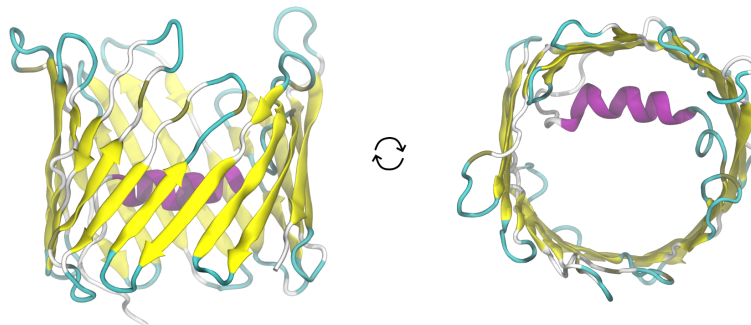


Figure 1: Illustration of the structure of human mitochondrial voltage-dependent anion channel [3]. The central alpha helix can move in or out of the pore, modulating the permeability to anions.

3 Significance

The goal of the proposed research is to improve the design process of transmembrane DNA nanostructures by quantitatively comparing a large number of prosthetic groups and morphologies. The usefulness of these comparisons will be demonstrated in the design and computational validation of a novel, gated, DNA

nanopore. To date, experimental methods have been held back by organic synthesis bottlenecks and associated costs while computational methods have been computationally expensive [20, 27, 33]. The expectation is that more life-like transmembrane structures will perform better than coarse-grained approximations. These hypotheses, however, require further refinement and validation.

Active research is being carried out to compare prosthetic groups more comprehensively such as the recent paper from the Aksimentiev group [20]. Their methods, however, rely on computationally intensive steered molecular dynamics and large, explicit systems. Our approach, in contrast, relies on free energy perturbation methods and well-defined sub-structures which will yield more quantitative, computationally cheaper results. Similarly, by repurposing alignment paradigms used in bioinformatics, we will use vector-valued, three-dimensional polar functions to quantitatively compare the surface morphologies of transmembrane proteins. We will then be able to back-map those morphologies to DNA nanoarchitectures making more exact mimics of the biological targets.

The end-product of this work will be (semi-)automated protocols for the design and assessment of DNA-membrane hybrid nanotechnologies including a curated library of parameterized prosthetic groups, programs to mathematically describe macromolecular surfaces, and refinements to existing free energy calculation methods. In the course of this research we will improve upon existing DNA nanoengineering methods, describe membrane inclusion morphologies, and be able to rank prosthetic groups and morphologies by their effects on membrane inclusions. These developments will facilitate future research in transmembrane nucleic acid structures as well as biopolymer nanotechnology generally by expanding the nanotechnologist's toolbox and providing design heuristics and methods for artificial membrane inclusions. It is hoped that these methods will also facilitate biochemical research into naturally occurring membrane inclusions by providing additional analysis methods for determining permeability, stability, and efficiency of transport proteins *in-silico*.

4 Preliminary Work

The preliminary research carried out so far can be divided into several distinct, though related, categories: assembly and manipulation of synthetic vesicles, assembly and characterization of DNA nanostructures, and modeling and simulation of DNA nanostructure/membrane systems.

4.1 DNA Nanostructures

Methods

DNA nanostructures ranged in size from a few dozen nucleotides (G-quadruplex) to over 14,000 nucleotides (DNA Origami). Structures were self-assembled using a standard annealing protocol (linear ramp from 90C to 15C over 10 hours) or by a short protocol (linear ramp from 90C to 15C over 1.5 hrs) depending on the size of the system. Post-annealing functionalization was achieved with a more moderate annealing protocol; either incubation at room temperature or a linear ramp from 37C to 15C over 1.5 hours. Assembly was carried out in Tris-Acetate/EDTA (TAE) buffer pH 7.5 with 12.5mM MgAc. Nanostructures were characterized variously by AFM (for large structures, Fig 3), poly-acrylamide gel electrophoresis (PAGE) (for smaller structures), and/or enzyme kinetics and FRET assays when appropriate (Figure 2).

Results and Discussion

4.2 Synthetic Vesicles

Methods

Giant-unilammellar POPC (palmitoyl-oleoyl-phosphatidylcholine) and POPC/PBD-b-PEG vesicles were produced by gel-assisted rehydration. First, agarose gel was dehydrated on the surface of a glass cover-slip. Then, stock solution of lipid/fluorophore in chloroform was spread thinly on the dry agarose and dried under vacuum. Finally, the dry lipid/agarose surface was rehydrated with a HEPES/sucrose buffer at 60C and imaged with fluorescence or confocal microscopy.

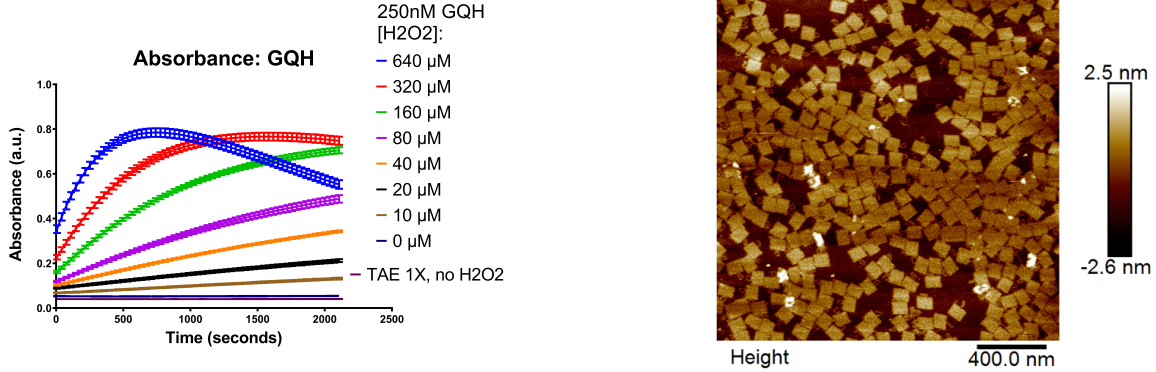


Figure 2: Sample enzymological data. Similar data can be used to quantify rates of transport across a synthetic membrane.

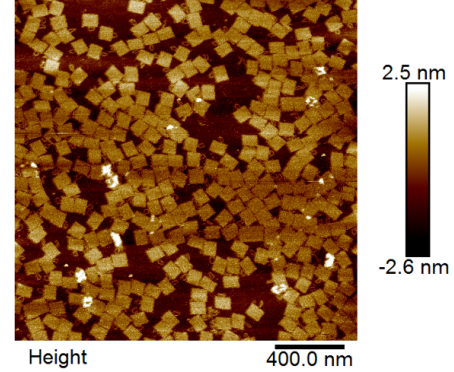


Figure 3: Sample rectangular DNA origami imaged using fluid AFM. Samples were annealed over 10hrs then imaged in TAE+Mg with zinc ions in solution to facilitate binding to the mica surface. Loops are individual helices 2.4nm in diameter.

Results and Discussion

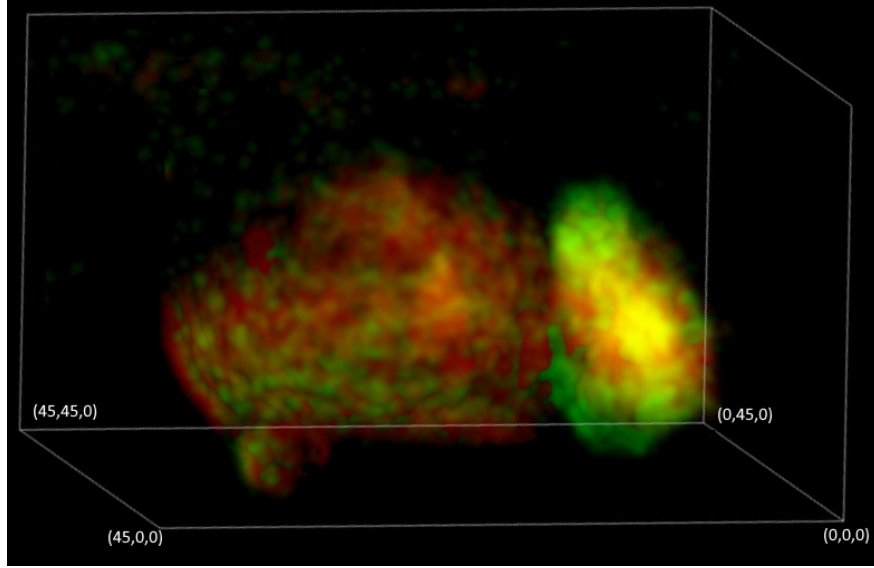


Figure 4: Confocal microscopy: 3D reconstruction of a hybrid synthetic vesicle (POPC:PBD-b-PEG) stained with nile red (generic lipophilic dye) and NBD-PC (green fluorophore, POPC analogue).

4.3 Modeling and Simulation

Parameterization of cholTEG-modified DNA

Although many biologically relevant molecules have already been parameterized in the CHARMM general forcefield, the diversity of bioconjugation chemistry is still being developed. As such, prosthetic groups must be parameterized primarily in-house. As a proof-of-concept, the most common prosthetic group, cholTEG, was parameterized along with a related prosthetic group which we call cholTEG' for convenience (it has a methyl instead of the short acyl chain on the carbon 20 of the cholesterol). This was achieved by subdividing

the prosthetic group into several smaller sections, some of which have already been parameterized (Figure 5); cholesterol, PEG monomer, and diethyl carbamate. Where necessary, methyl groups were replaced by methylene groups to allow connections between functional groups to create new residues. These new residues were then assembled (via custom patches) to the 3' end of a piece of DNA. Wherever possible, internal coordinates were preserved.

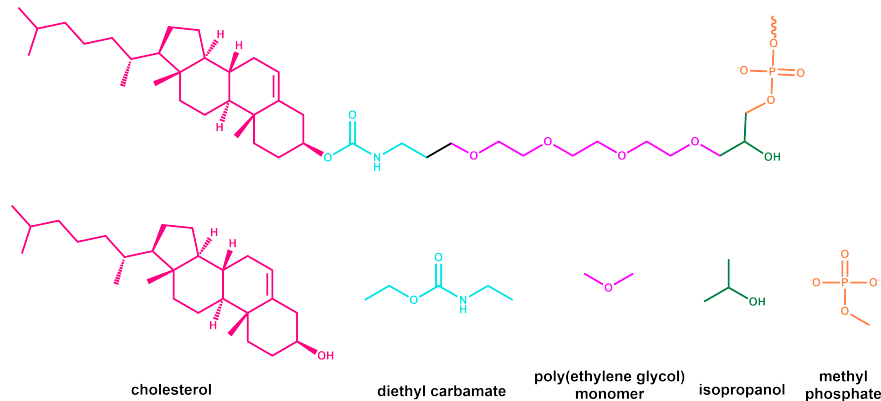


Figure 5: Schematic of cholTEG parameterization. The overall structure is divided into simpler 'monomers' which are then compared to the existing set of parameters. Modifications - most often from methyl to methylene - are made and unparameterized bonds are identified. The parameter set is completed by making analogies to existing parameters and validated in a series of simulations.

Once proper connectivity was confirmed, the small set of missing bond parameters were either generated by CGenFF utilities or manually by analogy to existing bonds in the lipid or nucleic acid parameter sets. Parameters were qualitatively validated by several short simulations - analogy penalties tended to be well below 15 (considered good, generally not requiring validation[cite]). [Plot of angle from normal]

FEP Mutation from Cholesterol to Cholesterol Analogue

A short double helix was patched to a POPC membrane and equilibrated at 300K for 85ns (Figure 6). The two most distal nucleotides were tethered together with a pseudobond to prevent dissociation of the two strands. Thus equilibrated, the cholesterol group of the cholTEG was mutated to cholesterol' using alchFEP and a dual topology. The acyl chain was decoupled while a methyl was coupled to replace it. The FEP calculation used 19 evenly spaced windows from lambda=0 to lambda=0.95 and 5 windows from 0.95 to 1. Each window had an equilibration time of 10ps and was run for 2ns.

5 Aim 1: Anchoring

To Identify Optimal Prosthetic Groups to Anchor DNA Nanostructures in Synthetic Membranes

5.1 Introduction and Summary

As noted in the introduction, cholTEG modification has enjoyed considerable popularity due to its commercial availability as a cell-uptake promoter - it is not, however, an ideal anchor for DNA transmembrane structures. The purpose of this aim, therefore, is to rank many prosthetic groups by their suitability as transmembrane anchors (including porphyrins, sterols, tocopherols, amino acid analogues, short polypeptides, and mono/di/tri-acyl glycerides). This will be achieved by free energy perturbations to predict relative free energies of patching and insertion which will be validate by fluorescence microscopy of a model system. Extending the WALP and KALP models, we expect the ideal anchor to satisfy, not only the hydrophobic demands, but the interfacial demands of the membrane as well.

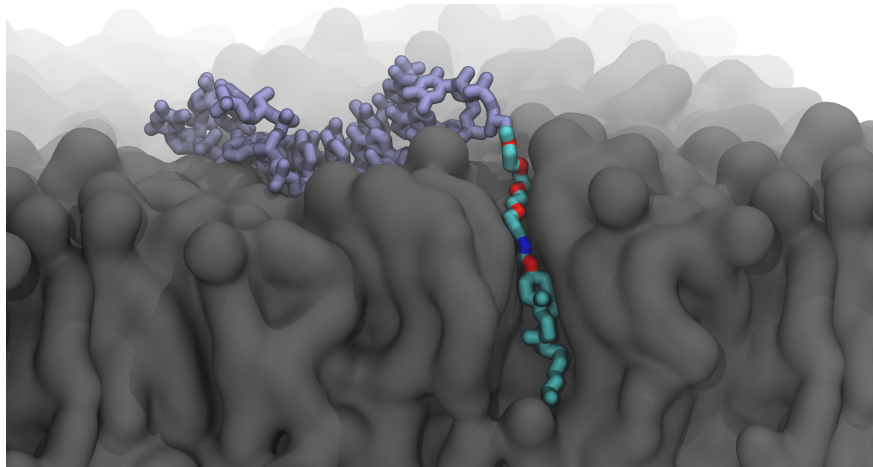


Figure 6: Still of DNA (light purple)-cholTEG (cyan=carbon, blue=nitrogen, red=oxygen) in a POPC membrane (gray, cutaway). Approximately 80ns of equilibration. Water and ions not shown for clarity.

5.2 Research Design

Aim 1.1: Distance Map of Prosthetic Groups

We can calculate the relative free energy of insertion much faster and more easily when comparing two similar prosthetic groups than two that are dissimilar. To that end, Tanimoto similarity scores will be used to generate a road map for the free energy perturbations and to facilitate more consistent parameterization.

The initial set of prosthetic groups will be taken directly from the existing literature so that direct, quantitative comparisons can be made. Additional prosthetic groups will be derived by analogy to biological and synthetic membrane-associated proteins and polypeptides (e.g. WALPeptides). More exotic prosthetic groups might include organometallics, unpaired nucleic acids, and nucleic acid analogues. Once identified, the prosthetic groups will be parameterized as needed using established CHARMM General Forcefield protocols - primarily by derivations from existing prosthetic groups. These manual parameterizations will be cross-referenced with ParamChem's automated CGenFF parameterization tool and validated against a combination of quantum calculations and experimental data from the literature as needed. The design of later computations and experiments will be structured by these initial findings.

Aim 1.2: Relative Free Energies of Insertion

Using the road map and parameterizations from aim 1.1, relative free energies of insertion for each prosthetic group will be computed using alchemical free energy perturbations. A simple model DNA inclusion will be used as the common substrate for these mutations which will consist of a six-helix bundle with prosthetic groups placed near the z-center. This will control for changes in the origami structure which would introduce errors in the FEP calculation. At least three membrane compositions will be used: POPC, POPC:DOPC:Chol, and PBD-b-PEG:POPC. These have been selected for their use experimentally.

In the interest of computational efficiency, we only consider those portions of the structure which are likely to interact directly with the membrane. To avoid denaturation of the complex, an initial set of whole-origami simulations will be carried out to determine an appropriate spring constant for a pseudobond holding the distal nucleotides together (as illustrated in preliminary data).

The membrane-inclusion system will be equilibrated for at least 100ns with the initial prosthetic group using the CHARMM36 and CGenFF in NAMD. Subsequent FEP calculations will be carried out using the same forcefield, parameters, and software using between 25 and 100 windows, 2ns each.

The data from these calculations are step-wise changes in free energy which are summed to find the overall difference in free energy. The Bennett Acceptance Ratio (BAR) estimator will be used to analyze

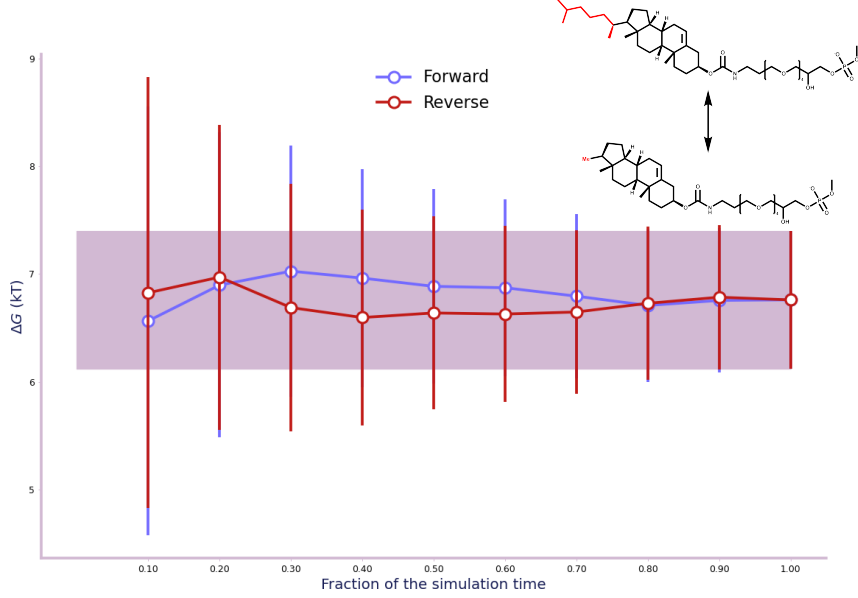


Figure 7: Change in free energy over the mutation from cholTEG to cholTEG'. The change in free energy over the mutation is approximately 6.76 kT or 4.01 kcal/mol. This will need to be compared to the mutation in water to determine the relative free energy of patching (as seen in Figure 9)

the data which will yield both a more accurate value of the relative free energy of solvation and approximate the associated error.

Following these computations, the most stable (energetically favorable) prosthetic groups will be identified for each membrane. The five to ten most stable prosthetic groups will be used in later aims. These results will be central to the larger goal of identifying optimal prosthetic groups and the design of transmembrane DNA nanostructures. We expect not only differences between prosthetic groups but also between membrane compositions - polymer-based membranes, especially, are likely to behave differently from more biological model membranes. As a result, and if time permits, we may also try computations involving a polymer-lipid hybrid membrane with some of the prosthetic groups to better understand the interaction between nanostructure, membrane, and prosthetic group.

The difference in free energy between the nanostructure in solution and the nanostructure associated with the membrane is related to the relative probabilities of those states via the Boltzmann distribution:

$$\frac{P_A}{P_B} = e^{\frac{-(E_A - E_B)}{k_B T}} \quad (1)$$

We can extend this to a three-state system (free, patched, inserted) by the following system of equations:

$$\frac{P_{\text{patched}}}{P_{\text{free}}} = e^{\frac{-(E_{\text{patched}} - E_{\text{free}})}{k_B T}} \quad (2)$$

$$\frac{P_{\text{patched}}}{P_{\text{inserted}}} = e^{\frac{-(E_{\text{patched}} - E_{\text{inserted}})}{k_B T}} \quad (3)$$

$$\frac{P_{\text{inserted}}}{P_{\text{free}}} = e^{\frac{-(E_{\text{inserted}} - E_{\text{free}})}{k_B T}} \quad (4)$$

However, if our empirical method cannot distinguish between the patched and inserted states, we must introduce a new variable: $P_{\text{associated}} = P_{\text{patched}} + P_{\text{inserted}} = 1 - P_{\text{free}}$

The above equations then yield:

$$\frac{P_{\text{Associated}}}{P_{\text{free}}} = \frac{P_{\text{patched}} + P_{\text{inserted}}}{P_{\text{free}}} \quad (5)$$

$$= \frac{P_{\text{patched}}}{P_{\text{free}}} + \frac{P_{\text{inserted}}}{P_{\text{free}}} \\ = e^{\frac{-(E_{\text{patched}} - E_{\text{free}})}{k_B T}} + e^{\frac{-(E_{\text{inserted}} - E_{\text{free}})}{k_B T}} \quad (6)$$

Where the relative free energies of patching and insertion can be estimated from FEP computations. Note that we are concerned only with the equilibrium state making the above derivation path-independent; we make no assumptions about the insertion pathway (cf. Figure 9).

5.3 Outline of Steps

Unless otherwise noted, all simulations will use the CHARMM36 forcefield with extensions based on CGenFF and run using NAMD. Simulations that include a membrane will be run for at least three membrane compositions: POPC, POPC:DOPC:Chol, PBD-b-PEG, possibly also PBD-b-PEG:POPC. Continuum models may be used throughout for time-saving sanity checks.

The aim will follow these general steps:

5.3.1 Aim 1.1: Select and Parameterize

Compile list of:

- all experimentally tested prosthetic groups
- all amino acid side-chains
- several lipid acyl chains
- 20 transmembrane polypeptides

Generate mol2 topologies

Organize Tanimoto similarity scores (or similar)

Semi-manually divide and parameterize

Create dual topologies based on organization

Run 10ns for each (five nt chain, pbc {20,20,20}) near the hydrophobic-solvent interface to check stability

5.3.2 Aim 1.2: Use FEP

Mutating along edges with at least X% similarity (an arbitrary cutoff) in solvent and membrane:

1. Among 10 experimentally tested prosthetic groups
2. Validate, cross-reference, refine work-flow
3. Among other experimentally tested prosthetic groups
4. Validate, cross-reference, refine work-flow
5. Among amino acid side-chains
6. Among lipid acyl chains

Grow polypeptide residue by residue up to 30 residues (twice as long as gramicidin)
 Mutate between the transmembrane polypeptides
 Rank by relative stability
 Calculate expected (relative) equilibrium loading

5.4 Expected Outcomes

At the completion of this aim, we expect to have a ranked data set that can be used to select prosthetic groups for future projects based on the membrane composition. Analyses will be confined to pairwise comparisons within specific membranes until enough data has been accumulated to justify (qualitative) comparisons between systems. Additional products will include: parameterizations for the prosthetic groups which can be used and adapted for later work; refinements to free energy perturbation methods; and a semi-automated pipeline for generating dual topologies.

5.5 Potential Problems and Alternative Approaches

Parameterization challenges

Parameterization of novel residues can frequently be achieved by a divide-and-conquer approach; the target is broken down into smaller sub-residues, compared to existing parameter sets, adjusted where necessary, and then recombined into the whole residue. Considerable effort has already been applied to the optimization of many parameter sets and only minimal validation is expected to be required. If, however, abnormal behaviors arise, we will resort to more rigorous parameterization protocols up to and including *ab-initio* quantum calculations.

FEP Accuracy and Efficiency

FEP computations are not expected to predict the exact free energies of insertion but rather the *relative* free energies so that comparisons can be made between prosthetic groups. As such, combination of the experimental and computational data will be necessary to make solid claims regarding the stability of any given prosthetic group. Internal consistency will be ensured using mutation cycles in which a prosthetic group is mutated $A \rightarrow B$, $B \rightarrow C$, and $C \rightarrow A$.

Given that the set of prosthetic groups is expected to reach approximately 100, the efficiency of computation is of concern. Initial benchmarking suggests that 20 to 30 ns per day can be achieved. If certain mutations are found to be particularly inefficient, we may resort to manual prosthetic group curation.

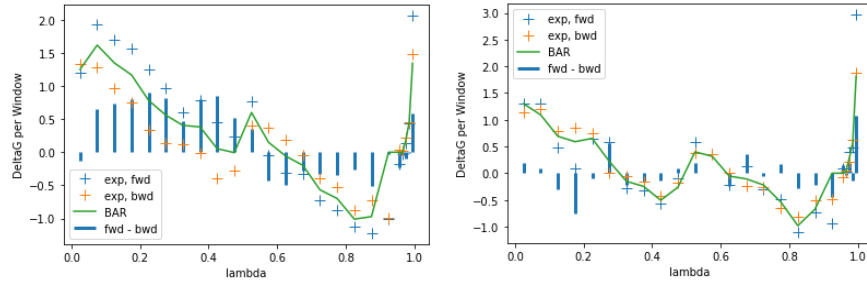


Figure 8: Examples of FEP calculations with (right) and without (left) full equilibration. Bars indicate the difference between forward (simulating state i, approximating state i+1) and backward (simulating state i+1, approximating state i) simulation.

Membrane/nanostructure instability

Instabilities in either DNA or membrane may require an extended equilibration period during which the membrane is expected to relax. Depending on the size, structure, and number of prosthetic groups, additional equilibration may be necessary. Disequilibrium is apparent in FEP calculations as illustrated in Figure 8. Estimated errors of more than 1kcal/mol can be addressed in several ways: 1) longer initial equilibration, 2) longer per-window equilibration, 3) longer sampling times, 4) smaller windows/non linear window sizes, 5) introduction of additional restraints to reduce orthogonal degrees of freedom which may have been introduced by sub-sectioning the DNA nanostructure. An alternative to subsectioning of the DNA nanostructure would be to extend it beyond the periodic boundaries; i.e. the DNA would be modeled as *infinitely long* helices.

6 Aim 2: Morphology

To Optimize Nanostructure Morphology Including Position and Number of Prosthetic Groups

6.1 Introduction and Summary

Suboptimal morphology is a major source of cytotoxicity and leakiness of transmembrane DNA nanostructures. To improve upon existing designs, we will systematically test and compare the permeability and stability of several inclusion morphologies derived from biological systems. We hypothesize that an appropriate combination of shape and prosthetic group placement will minimize leakiness and membrane disruption.

An attractive solution would be to directly combine the membrane-facing region of a protein with a DNA nanostructure, but this presents several engineering problems. First, protein structure is not modular, but integral - separating the outer residues from the interior is very likely to completely alter the tertiary structure. Second, even if such a protein annulus could be synthesized or isolated, selective covalent attachment to an already-assembled DNA nanostructure would require extensive development if it is even possible in this formulation. Finally, even once such a process was developed, it would require multiple steps and be difficult to scale to production. Rather, modular conjugation of prosthetic groups to oligonucleotides which are then assembled with well-established procedures is the method most likely to succeed given the current state of the art.

This larger goal will be achieved by comparing inclusion geometries in two ways: first, using carefully constrained coarse-grained model DNA/polyanion inclusions (Martini and Gromacs); and second, using all-atom models (CHARMM and NAMD). We will leverage existing models of transmembrane proteins and combine those with DNA nanotechnology to work toward optimal architectures. Although we are unlikely to remove all undesirable effects, we do hope to reduce these significantly and be able to compare novel architectures to already-characterized designs.

6.2 Research Design

Aim 2.1 Approximate life-like inclusions using DNA nanotechnology

The main deliverable for this subaim will be a set of DNA nanoarchitectures which incorporate what is already known about naturally occurring membrane inclusions. Having generated a list of prosthetic groups and having several target morphologies (selected from well-studied membrane proteins and one or two de-novo structures), design will be carried out in two steps: 1) fill the bulk of the shape with DNA double helices, 2) introduce two or more prosthetic groups to produce a hydrophobic domain.

Aim 2.2 Compare the Stabilities and Permeability of each Inclusion

Each of the resulting structures from 2.1 will be simulated using classical MD in a membrane to check for stability in both coarse-grained and all-atom models; unstable inclusions will disrupt the membrane, resist

equilibration, and may even dissociate from the membrane entirely. An unmodified origami will be used as a negative control. These results will be used to validate, justify, or modify the approximations made up to this point. Longer CG simulations will be used to estimate solvent and ion permeability of each membrane inclusion; validated with all-atom well-tempered metadynamics (in which a the free energy surface in and around the nanostructure is sampled).

Aim 2.3 Compare the relative free energies of insertion for each morphology

Unlike prosthetic group free energies of mutation, there is no direct computational (or chemical) transformation from one inclusion geometry to another. Rather, whole inclusions will be decoupled from the simulation. Such calculations are likely to converge slowly and we may also attempt modifications to standard alchemical perturbations (lambda dynamics) such as decoupling the inclusion in layers or treating each intermolecular force independently. One possibility would be to decouple the molecular structure leaving an idealized cavity which can then be handled by thermodynamic integration (shrunken step-wise). Metadynamics, a more established method, will be used for comparison in a subset of cases due to its considerable computational cost.

These results will make it possible to select optimal geometries and the methods can be extended to related systems. These calculations will be carried out first using a coarse-grained model (Martini) then validated using an all-atom model (CHARMM).

6.3 Outline of Steps

Unless otherwise noted, all simulations will use the CHARMM36 forcefield with extensions based on CGenFF and run using NAMD. Coarse grained simulations will use Martini3 run in Gromacs. Simulations that include a membrane will be run for at least three membrane compositions: POPC, POPC:DOPC:Chol, PBD-b-PEG, possibly also PBD-b-PEG:POPC. Continuum models may be used throughout for time-saving sanity checks. Modeling and design will use a combination of caDNAno, oxDNA, and VMD/Tcl.

The aim will follow these general steps:

6.3.1 Aim 2.1: Design the Inclusions with DNA

Select a set of about six inclusion morphologies both strictly biological and life-inspired
Manually approximate the underlying structures with DNA nanostructures
Manually approximate the hydrophobic surfaces with prosthetic groups

6.3.2 Aim 2.2: Compare morphology stability and permeability

Use coarse-grained and all-atom simulations to check stability and internal stress
Use coarse-grained simulation to estimate ion and water permeability
Use all-atom metadynamics to validate the CG permeability estimates

6.3.3 Aim 2.3: Estimate free energies of insertion using FEP

Using first CG, then AA models:

1. Attempt complete decoupling of small inclusion
2. Compare to a two-step Chandler solvation calculation
3. Compare to a traditional metadynamics calculation

Continue with the most time-efficient method balancing accuracy and computational cost
Compute the free energy of insertion for each of the inclusions

6.4 Expected Outcomes

Once this aim has been met we expect to have 1) an improved methodologies for comparing macromolecular membrane inclusions computationally and 2) a set of DNA nanostructures organized by stability and permeability metrics. We further hope to identify morphologies which minimize leakiness of transmembrane DNA nanostructures rivalling natural transmembrane proteins. Based on work by Aksimentiev and colleagues [31], we do expect some degree of membrane disruption, but remain optimistic about the prospect of minimizing this. Furthermore, by comparison to polypeptide membrane inclusions, it is expected that the thickness and shape of the hydrophobic domain will play a significant role in stability of the inclusion and the degree of membrane disruption. Membrane disruption will be quantified by the distance of the lipid head groups from the midplane and from the interleaflet interface. These optimizations will provide bases on which DNA nanotechnologists will be able to build.

6.5 Potential Problems and Alternative Approaches

The results from Aksimentiev, Howorka, and others suggest that at least two prosthetic groups are necessary to stabilize a transmembrane inclusion. More may be helpful but incur a greater experimental cost. The number of prosthetic groups will not be capped, but optimization will be attempted to minimize the number of chemical modifications.

It may be that FEP and metadynamics will fail to converge for free energy calculations. In this case, we may resort to spatial methods such as adaptive biasing force, or umbrella sampling. Comparisons to existing experimental data will be made where possible including results from patch clamp current measurements, order parameters, and permeability measurements.

7 General Computational Methods

7.1 Molecular Dynamics

7.1.1 General Description

Classical molecular dynamics numerically applies Newton's laws to molecular systems. Atoms (or groups of atoms) are approximated as spherical particles with mass, charge, Van der Waals radii, etc. Electron interactions are approximated with a system of idealized springs - quantum electrodynamics are not solved explicitly. As a result of these constraints, classical MD is best suited to studying conformational and diffusive dynamics. At the lowest level of abstraction (called all-atom simulations), a typical system will consist of 500,000 to 2,000,000 atoms (10 to 20nm per side) and reach timescales on the order of several hundred nanoseconds. More abstract simulations (called coarse-grained) model groups of atoms and can reach timescales on the order of microseconds. While energy is known (and required) for each simulation step, *free* energy requires sampling of every configuration in a given state which would take much too long using molecular dynamics alone. For this reason so-called enhanced sampling methods, such as free energy perturbations and metadynamics, are used to describe the free energy landscape along one or more reaction coordinates (see below).

The proposed course of research will involve all-atom simulations (CHARMM36 with cation-pi corrections, magnesium hexahydrate, and run with NAMD) to predict the diffusive dynamics of small molecules and ions in and around the transmembrane nanostructures. As a computational microscope and detailed model, MD simulations will allow us to make and understand adjustments to nanostructure design without the need to physically prototype every modification. We can also gain insight into the conformational stability of the nanostructure and associated pore including deformations in the membrane and the electromechanical forces at play.

7.1.2 Specifics

Simulations will be run using the CHARMM36 forcefield. Where possible, prosthetic groups are parameterized by making small changes to existing residues (e.g. replacing a methyl group, CG331 and HGA3, with

a methylene, CG321 and HGA2). More complex prosthetic groups may require use of CGenFF tools like ParamChem or CHARMM-GUI's ligand modeler, but these parameter sets sometimes require optimization and don't always account for resonance structures. Parameters for membrane lipids and DNA are well established, but cation-DNA parameterizations are still debated. We will make some comparisons between simulations carried out with magnesium hexahydrate and pure sodium chloride.

Judicious application of pseudobonds should allow us to reduce the overall number of atoms required to fully describe the systems of interest. Current simulations in membrane and solution consist of approximately 500,000 atoms which can be run at about 20ns per day on Amarel CPUs. Simulations of over 100ns are well within reach with room for growth if needed.

7.2 Free Energy Perturbations

7.2.1 General Description

Free energy perturbations (FEP) are an extension of molecular dynamics simulations in which a system at equilibrium is slowly transformed to a modified system and the resulting change in free energy is calculated. This is achieved by turning off the non-bonded interactions of the unique atoms in the initial system while turning on interactions of the unique atoms of the target system. It is the computational analogue to end-point concentration measurements from which we can calculate changes in free energy by the Zwanzig Equation (Equation 7), which states: for any two sufficiently similar macrostates, the difference in free energy is the natural logarithm of the mean relative Boltzmann weight of the second macrostate averaged over the microstates of the first macrostate.

$$\Delta F = -\frac{1}{\beta} \ln \left\langle e^{-\beta[E_b - E_a]} \right\rangle_a \quad (7)$$

Where F is the Helmholtz free energy, β is $k_B T$, E_x is the energy of state x , and angle brackets indicate the average over the ensemble of microstates in some macrostate (a or b). The states of interest (prosthetic group a or b) are unlikely to converge in a reasonable amount of time; instead we sum over a set of smaller perturbations to approximate the larger change [46]. This is conveniently expressed using a coupling parameter, λ :

$$\Delta F = \sum_{\lambda_i=0}^1 \ln \left\langle \exp [-\beta[E_{\lambda_{i+1}} - E_{\lambda_i}]] \right\rangle_\lambda \quad (8)$$

Where λ_i is zero in the initial state, a, and one in the final state, b. This method can be used, not only to estimate ΔG of a chemical reaction, but also to estimate free energies of solvation and to compare the solubility of chemical species.

The alchemical FEP calculations operate by slowly transforming ("mutating") one prosthetic group to another. The relative free energy of insertion can be derived from the difference between free energy of mutation in solution and in the membrane as seen in Equation 9 and illustrated in Figure 9.

$$\Delta F_{mem} - \Delta F_{aq} = \frac{\Delta F_A}{A \rightarrow B} - \frac{\Delta F_B}{A \rightarrow B} \quad (9)$$

7.2.2 Specifics

Dual-topology systems will be equilibrated for 100ns prior to FEP computations. Twenty-five to one hundred non-uniform lambda windows of 2ns each will be used initially (plus 10ps of equilibration for each window). Equilibration time(s) and window widths will be adjusted if poor convergence is observed. FEP computations will make use of Interleaved Double-Wide Sampling to improve efficiency and data will be decorrelated to reduce background signal. A small set of test runs will be carried out to determine if embarrassingly parallel simulation of windows improves overall compute time without sacrificing accuracy.

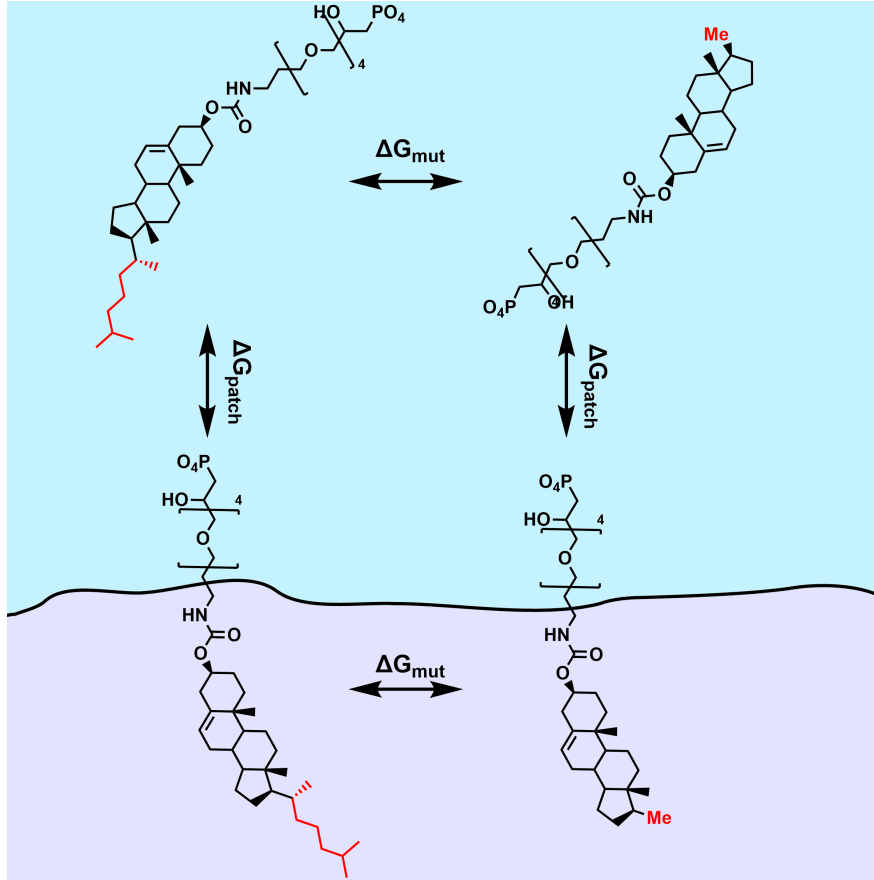


Figure 9: Illustration of a thermodynamic cycle. The relative free energy of insertion is equal to the difference between the free energies of mutation (Eq. 9)

7.3 Metadynamics

7.3.1 General Description

Metadynamics is an enhanced sampling technique in which the system is allowed to explore the energy landscape in a self-avoiding way. By this we mean that the simulation will tend not to visit very similar conformations multiple times [figure illustrating exploration of the energy landscape]. In this way it becomes possible to explore the energy landscape far from the global minimum (e.g. near some rare event for example). This is achieved by applying an artificial potential¹:

$$V_G(S, t) = w \sum_{t'=\tau_G, 2\tau_G}^t \exp\left(\frac{-(S - s(t'))^2}{2\delta s^2}\right) \quad (10)$$

Which approximates the free energy landscape in the limit:

$$\lim_{t \rightarrow \infty} V_G(S, t) = -F(S) + C \quad (11)$$

Well-tempered metadynamics is a modification in which the temperature is gradually increased to improve sampling of the local energetic minima at the expense of energetic maxima (which make little contribution to the 'average' state).

¹w is the weight of the Gaussian, δs is the width, τ_G is the time interval between depositions, t is time, S is the value of the collective variable, and $s(t) = S(x(t))$

7.3.2 Specifics

The collective variable will be initially defined as the distance of the nanoparticle from the XY center of the pore. If this is found to be inadequate to capture the dynamics of the system, we will adjust the CV to be the polar coordinates of the nanoparticle from the particle's center in the 'closed' conformation. The closed conformation for this purpose will be defined as the closest point the nanoparticle can approach the XYZ center of the pore without disrupting the nanostructure.

Approximately 50ns of equilibration followed by $5\mu\text{s}$ of simulation time should be adequate to sample the energetic landscape. Standard procedures will be used to determine if additional equilibration is needed. The largest system is expected to be about 750,000 atoms. University computing resources should be capable of completing these simulations at a rate of about 100ns per week.

8 Timeline

Summer 2021: Aim 1.1
Fall 2021: Aim 1.1
Spring 2022: Aim 1.2
Summer 2022: Aim 1.2, begin 2.1
Fall 2022: Aim 2.1
Spring 2023: Aim 2.2
Summer 2023: Aim 2.2
Fall 2023: Aim 2.3
Spring 2024: Aim 2.3

References

- [1] Elif Turker Acar, Steven F. Buchsbaum, Cody Combs, Francesco Fornasiero, and Zuzanna S. Siwy. Biomimetic potassium-selective nanopores. *Science Advances*, 5(2):eaav2568, feb 2019.
- [2] Milan Balaz, Andrea E. Holmes, Michele Benedetti, Pamela C. Rodriguez, Nina Berova, Koji Nakanishi, and Gloria Proni. Synthesis and circular dichroism of tetraarylporphyrin-oligonucleotide conjugates. *Journal of the American Chemical Society*, 127(12):4172–4173, mar 2005.
- [3] M. Bayrhuber, T. Meins, M. Habeck, S. Becker, K. Giller, S. Villinger, C. Vonrhein, C. Griesinger, M. Zweckstetter, and K. Zeth. Structure of the human voltage-dependent anion channel, oct 2008.
- [4] Oliver Birkholz, Jonathan R. Burns, Christian P. Richter, Olympia E. Psathaki, Stefan Howorka, and Jacob Piehler. Multi-functional dna nanostructures that puncture and remodel lipid membranes into hybrid materials. *Nature Communications*, 9, 2018. 1521 33 29670084.
- [5] Jonathan R. Burns, Noura Al-Juffali, Sam M. Janes, and Stefan Howorka. Membrane-spanning dna nanopores with cytotoxic effect. *Angewandte Chemie-International Edition*, 53(46):12466–12470, 2014. SI 64 25294680.
- [6] Jonathan R. Burns, Kerstin Goepfrich, James W. Wood, Vivek V. Thacker, Eugen Stulz, Ulrich F. Keyser, and Stefan Howorka. Lipid-bilayer-spanning dna nanopores with a bifunctional porphyrin anchor. *Angewandte Chemie-International Edition*, 52(46):12069–12072, 2013. 127 24014236.
- [7] Jonathan R. Burns and Stefan Howorka. Structural and functional stability of dna nanopores in biological media. *Nanomaterials*, 9(4), 2019. 490 7 30934927.
- [8] Jonathan R. Burns, Astrid Seifert, Niels Fertig, and Stefan Howorka. A biomimetic dna-based channel for the ligand-controlled transport of charged molecular cargo across a biological membrane. *Nature Nanotechnology*, 11(2):152–156, 2016. 173 26751170.

- [9] Jonathan R. Burns, Eugen Stulz, and Stefan Howorka. Self-assembled dna nanopores that span lipid bilayers. *Nano Letters*, 13(6):2351–2356, 2013. 172 23611515.
- [10] Liang Chen, Siping Liang, Yu Chen, Minhao Wu, and Yuanqing Zhang. Destructing the plasma membrane with activatable vesicular DNA nanopores. *ACS Applied Materials & Interfaces*, 12(1):96–105, dec 2019.
- [11] Zhaowei Chen, Zejun Wang, and Zhen Gu. Bioinspired and biomimetic nanomedicines. *Accounts of Chemical Research*, apr 2019.
- [12] Es Darley, Jasleen Kaur Daljit Singh, Natalie A. Surace, Shelley F. J. Wickham, and Matthew A. B. Baker. The fusion of lipid and DNA nanotechnology. *Genes*, 10(12):1001, dec 2019.
- [13] S. Dorairaj and T. W. Allen. On the thermodynamic stability of a charged arginine side chain in a transmembrane helix. *Proceedings of the National Academy of Sciences*, 104(12):4943–4948, mar 2007.
- [14] Debasis Ghosh, Lakshmi P Datta, and Thimmaiah Govindaraju. Molecular architectonics of DNA for functional nanoarchitectures. *Beilstein Journal of Nanotechnology*, 11:124–140, jan 2020.
- [15] Guilhem Godeau, Cathy Staedel, and Philippe Barthélémy. Lipid-conjugated oligonucleotides via “click chemistry” efficiently inhibit hepatitis c virus translation. *Journal of Medicinal Chemistry*, 51(15):4374–4376, jul 2008.
- [16] Thimmaiah Govindaraju. *Templated DNA nanotechnology : functional DNA nanoarchitectonics*. Pan Stanford Publishing, Singapore, 2019. edited by Thimmaiah Govindaraju.
- [17] Lei Guo, Shunfang Wang, Mingyuan Li, and Zicheng Cao. Accurate classification of membrane protein types based on sequence and evolutionary information using deep learning. *BMC Bioinformatics*, 20(S25), dec 2019.
- [18] Stefan Howorka. Building membrane nanopores. *Nature Nanotechnology*, 12(7):619–630, jul 2017.
- [19] Shuaidong Huo, Hongyan Li, Arnold J. Boersma, and Andreas Herrmann. DNA nanotechnology enters cell membranes. *Advanced Science*, 6(10):1900043, mar 2019.
- [20] Sioned F. Jones, Himanshu Joshi, Stephen J. Terry, Jonathan R. Burns, Aleksei Aksimentiev, Ulrike S. Eggert, and Stefan Howorka. Hydrophobic interactions between DNA duplexes and synthetic and biological membranes. *Journal of the American Chemical Society*, 143(22):8305–8313, may 2021.
- [21] Elizabeth Jurrus, Dave Engel, Keith Star, Kyle Monson, Juan Brandi, Lisa E. Felberg, David H. Brookes, Leighton Wilson, Jiahui Chen, Karina Liles, Minju Chun, Peter Li, David W. Gohara, Todd Dolinsky, Robert Konecný, David R. Koes, Jens Erik Nielsen, Teresa Head-Gordon, Weihua Geng, Robert Krasny, Guo-Wei Wei, Michael J. Holst, J. Andrew McCammon, and Nathan A. Baker. Improvements to the APBS biomolecular solvation software suite. *Protein Science*, 27(1):112–128, oct 2017.
- [22] R. R. Ketcham, K. C. Lee, S. Huo, and T. A. Cross. Macromolecular structural elucidation with solid-state nmr-derived orientational constraints, 1996.
- [23] J. Antoinette Killian. Synthetic peptides as models for intrinsic membrane proteins. *FEBS Letters*, 555(1):134–138, oct 2003.
- [24] Swati Krishnan, Daniela Ziegler, Vera Arnaut, Thomas G. Martin, Korbinian Kapsner, Katharina Henneberg, Andreas R. Bausch, Hendrik Dietz, and Friedrich C. Simmel. Molecular transport through large-diameter DNA nanopores. *Nature Communications*, 7(1), sep 2016.
- [25] M. Langecker, V. Arnaut, T. G. Martin, J. List, S. Renner, M. Mayer, H. Dietz, and F. C. Simmel. Synthetic lipid membrane channels formed by designed DNA nanostructures. *Science*, 338(6109):932–936, nov 2012.

- [26] Domenico Lombardo, Mikhail A. Kiselev, and Maria Teresa Caccamo. Smart nanoparticles for drug delivery application: Development of versatile nanocarrier platforms in biotechnology and nanomedicine. *Journal of Nanomaterials*, 2019:1–26, feb 2019.
- [27] Vishal Maingi, Mickaël Lelimousin, Stefan Howorka, and Mark S. P. Sansom. Gating-like motions and wall porosity in a DNA nanopore scaffold revealed by molecular simulations. *ACS Nano*, 9(11):11209–11217, oct 2015.
- [28] Emily Mastronardi, Amanda Foster, Xueru Zhang, and Maria DeRosa. Smart materials based on DNA aptamers: Taking aptasensing to the next level. *Sensors*, 14(2):3156–3171, feb 2014.
- [29] Eszter E. Najbauer, Stefan Becker, Karin Giller, Markus Zweckstetter, Adam Lange, Claudia Steinem, Bert L. de Groot, Christian Griesinger, and Loren B. Andreas. Structure, gating and interactions of the voltage-dependent anion channel. *European Biophysics Journal*, 50(2):159–172, mar 2021.
- [30] David Nelson. *Lehninger principles of biochemistry*. W.H. Freeman and Company Macmillan Higher Education, New York, NY Hounds mills, Basingstoke, 2017.
- [31] Alexander Ohmann, Chen-Yu Li, Christopher Maffeo, Kareem Al Nahas, Kevin N. Baumann, Kerstin Göpfrich, Jejoong Yoo, Ulrich F. Keyser, and Aleksei Aksimentiev. A synthetic enzyme built from DNA flips 107 lipids per second in biological membranes. *Nature Communications*, 9(1), jun 2018.
- [32] Thomas D. Pollard, William C. Earnshaw, Jennifer Lippincott-Schwartz, and Graham Johnson. *Cell Biology*. Elsevier LTD, Oxford, January 2017.
- [33] Erik Poppleton, Joakim Bohlin, Michael Matthies, Shuchi Sharma, Fei Zhang, and Petr Šulc. Design, optimization and analysis of large DNA and RNA nanostructures through interactive visualization, editing and molecular simulation. *Nucleic Acids Research*, 48(12):e72–e72, may 2020.
- [34] Mahmudur Rahman, Mohammad Julker Neyen Sampad, Aaron Hawkins, and Holger Schmidt. Recent advances in integrated solid-state nanopore sensors. *Lab on a Chip*, 2021.
- [35] Milton H Saier, Vamsee S Reddy, Gabriel Moreno-Hagelsieb, Kevin J Hendargo, Yichi Zhang, Vasu Iddamsetty, Katie Jing Kay Lam, Nuo Tian, Steven Russum, Jianing Wang, and Arturo Medrano-Soto. The transporter classification database (TCDB): 2021 update. *Nucleic Acids Research*, 49(D1):D461–D467, nov 2020.
- [36] Milton H. Saier, Vamsee S. Reddy, Dorjee G. Tamang, and Åke Västermark. The transporter classification database. *Nucleic Acids Research*, 42(D1):D251–D258, nov 2013.
- [37] Astrid Seifert, Kerstin Göpfrich, Jonathan R. Burns, Niels Fertig, Ulrich F. Keyser, and Stefan Howorka. Bilayer-spanning DNA nanopores with voltage-switching between open and closed state. *ACS Nano*, 9(2):1117–1126, dec 2014.
- [38] Qi Shen, Michael W. Grome, Yang Yang, and Chenxiang Lin. Engineering lipid membranes with programmable DNA nanostructures. *Advanced Biosystems*, 4(1):1900215, dec 2019.
- [39] Wenqing Shi, Alicia K. Friedman, and Lane A. Baker. Nanopore sensing. *Analytical Chemistry*, 89(1):157–188, nov 2017.
- [40] Christian Sigl, Elena M. Willner, Wouter Engelen, Jessica A. Kretzmann, Ken Sachenbacher, Anna Liedl, Fenna Kolbe, Florian Wilsch, S. Ali Aghvami, Ulrike Protzer, Michael F. Hagan, Seth Fraden, and Hendrik Dietz. Programmable icosahedral shell system for virus trapping. *Nature Materials*, 2021.
- [41] Friedrich C. Simmel, Bernard Yurke, and Hari R. Singh. Principles and applications of nucleic acid strand displacement reactions. *Chemical Reviews*, 119(10):6326–6369, 2019. SI 129 30714375.
- [42] Eugen Stulz. Nanoarchitectonics with porphyrin functionalized DNA. *Accounts of Chemical Research*, 50(4):823–831, mar 2017.

- [43] Janos Szebeni and Rudolf Urbanics. Complement activation-related pseudoallergy caused by nanomedicines and its testing in vitro and in vivo. pages 109–114, nov 2011.
- [44] Rasmus P. Thomsen, Mette Galsgaard Malle, Anders Hauge Okholm, Swati Krishnan, Søren S.-R. Bohr, Rasmus Schøler Sørensen, Oliver Ries, Stefan Vogel, Friedrich C. Simmel, Nikos S. Hatzakis, and Jørgen Kjems. A large size-selective DNA nanopore with sensing applications. *Nature Communications*, 10(1), dec 2019.
- [45] Ailing Tong, John T Petroff, Fong-Fu Hsu, Philipp AM Schmidpeter, Crina M Nimigean, Liam Sharp, Grace Brannigan, and Wayland WL Cheng. Direct binding of phosphatidylglycerol at specific sites modulates desensitization of a ligand-gated ion channel. *eLife*, 8, nov 2019.
- [46] Mark Tuckerman. *Statistical Mechanics: Theory and Molecular Simulation*. OXFORD UNIV PR, April 2010.
- [47] Mingxu You, Yifan Lyu, Da Han, Liping Qiu, Qiaoling Liu, Tao Chen, Cuichen Sam Wu, Lu Peng, Liqin Zhang, Gang Bao, and Weihong Tan. DNA probes for monitoring dynamic and transient molecular encounters on live cell membranes. *Nature Nanotechnology*, 12(5):453–459, mar 2017.